International Journal of Mathematical Archive-4(11), 2013, 203-215
Available online through www.ijma.info ISSN 2229 – 5046

SORET AND DUFOUR EFFECTS ON MIXED CONVECTION HEAT AND MASS TRANSFER WITH VARIABLE FLUID PROPERTIES

N. Nalinakshi[1*], P. A. Dinesh[2] and D. V. Chandrashekhar[3]

[1]Dept. of Mathematics, Atria Institute of Technology, Bangalore, India.

[2]Dept. of Mathematics, M. S. Ramaiah Institute of Technology, Bangalore, India.

[3]Dept. of Mathematics, Vivekananda Institute of Technology, Bangalore, India.

(Received on: 14-10-13; Revised & Accepted on: 16-11-13)

ABSTRACT

A *Numerical approach has been carried out for the study of Soret and Dufour effects on mixed convection heat and mass transfer past a vertical heated plate embedded in a Newtonian fluid saturated sparsely packed porous medium with variable fluid properties such as variable porosity, permeability and thermal conductivity. The boundary layer flow in the porous medium is governed by Lapwood-Brinkmann extended Darcy model. Similarity transformations are employed and the resulting ordinary differential equations are solved using shooting technique with Runge–Kutta-Fehlberg scheme to obtain velocity, temperature and concentration distributions. The features of fluid flow, heat and mass transfer characteristics are analyzed by plotting the graphs and the physical aspects are discussed in detail to interpret the effect of various significant parameters of the problem. The results obtained show that the impact of buoyancy ratio parameter (N), Soret number (S_r), Dufour number (D_f), Prandtl number (Pr), Schmidt number (Sc) and other parameters plays an important role in the fluid flow through porous medium. Further, the obtained results under the limiting conditions were found to be in good agreement with the existing results.*

Keywords*: Newtonian fluid; vertical heated plate; porous media; Mixed convection; shooting technique.*

1. INTRODUCTION

Soret and Dufour effects are interesting macroscopically the physical phenomenon in fluid mechanics, when heat and mass transfer occur simultaneously in a moving fluid, the relation between the fluxes and the driving potentials are of more intricate nature. It has been found that an energy flux can be generated not only by temperature gradients but by composition gradients as well. The heat transfer caused by concentration gradient is called the diffusion-thermo or Dufour effect. On the other hand, mass transfer caused by temperature gradients is called Soret or thermal diffusion effect. Thus soret effect is referred to species differentiation developing in an initial homogeneous mixture submitted to a thermal gradient and the Dufour effect referred to the heat flux produced by a concentration gradient. The effect of the Dufour parameter on the local surface temperature becomes more significant and the effect of Soret parameter leads to an increase in the local surface concentration.

In most of the studies related to heat and mass transfer process, soret and Dufour effects are neglected on the basis that they are of a smaller order of magnitude than the effects described by Fourier's and Fick's laws. But these effects are considered as second order phenomena and may become significant in areas such as hydrology, petrology, geosciences, etc. The soret effect, for instance, has been utilized for isotope separation and in mixture between gases with very light molecular weight and of medium molecular weight. The Dufour effect was recently found to be of order of considerable magnitude so that it cannot be neglected (see Eckert and Drake [9]). Several authors have studied the problem of mixed convection about different surface geometrics. The analysis of convective transport in a porous medium with the inclusion of non–Darcian effects has also been a matter of study in recent years. The inertia effect is expected to be important at a higher flow rate and it can be accounted for through the addition of a velocity squared term in the momentum equation, which is known as the Forchheimer's extension of the Darcy's law. A detailed review of convective heat transfer in Darcy and non-Darcy porous medium can be found in the book by Nield and Bejan [15].

Corresponding author: N. Nalinakshi[1]*
[1]Dept. of Mathematics, Atria Institute of Technology, Bangalore, India.

Anghel *et al* [2] investigated the Dufour and Soret effects on free convection boundary layer over a vertical surface embedded in a porous medium. Recently, Postelnicu [17] studied numerically the Influence of magnetic field on heat and mass transfer by natural convection from vertical surfaces in porous media considering Soret and Dufour effects. Govardhan *et al* [12] has analyzed the effect of soret and Dufour effects on MHD free convection Heat and Mass transfer in a Doubly stratified darcy porous medium with viscous dissipation and found that and Soret and Dufour effects are receiving much attention with velocity, temperature and concentration of the fluids. Gnaneswara and Bhaskar [10] studied Soret and Dufour effects on steady MHD free convection flow past a semi infinite moving vertical plate in a porous medium with viscous dissipation and analysis that effect of Dufour and Soret numbers rises in the skin friction coefficient whereas rise in Sherwood number and fall in Nusselt number and rise in Nusselt number and fall in the Sherwood number respectively. Hence Soret and Dufour effects cannot be neglected. Later Gnaneswara and Bhaskar [11] made finite element analysis of Soret and Dufour effects on unsteady MHD free convection flow past an impulsively started vertical porous plate with viscous dissipation.

Alam and Rahman [1] made numerical study of the Dufour and Soret effects on mixed convection flow past a semi-infinite vertical flat plate embedded in a porous medium using the Brinkman model, who found that wall suction reduces the boundary layer velocity, the thermal and also the solute concentration growth. Balasubrahmanyam et al [4] examines the Soret effect on mixed convective heat and mass transfer through a porous medium confined in a cylindrical annulus under a radial magnetic field in the presence of a constant heat source / sink. The Double-diffusive convection in a horizontal layer work including inertial effects was made by Awad *et al* [3] using the modified Darcy-Brinkman model to investigate double diffusive convection in a Maxwell fluid in the presence of Dufour and Soret effects in a highly porous medium.

In some industrial applications, such as fixed-bed catalytic reactors, packed bed heat exchangers and drying, the value of the porosity is maximum at the wall and minimum away from the wall, so the porosity of the porous medium should be taken as non – uniform. Porosity measurements by Shwartz and Smith [18] and Benenati and Brosilow [5] show that porosity is not constant but varies from the wall to the interior of the porous medium due to which permeability also varies. Chandrasekhara *et al* [6, 7] has incorporated the variable permeability to study the flow past and through a porous medium and have shown that the variation of porosity and permeability has greater influence on velocity distribution and on heat transfer. Nevertheless, the inertia effects become important in a sparsely packed porous medium and hence their effect on mixed convection problems needs to be investigated. Mohammadein and El-shaer [13] studied mixed convective flow past a semi-infinite vertical plate embedded in a porous medium incorporating the variable permeability in Darcy's model. Recently, Pal and Shivakumar [16] analyzed mixed convection heat transfer from a vertical heated plate embedded in a Newtonian fluid sparsely packed porous medium by considering the variation of permeability, porosity and thermal conductivity. Dulal Pal [8] studied magneto hydrodynamic non-Darcy mixed convection heat transfer from a vertical heated plate embedded in a porous medium with variable porosity, by taking the viscous dissipation term in the energy equation. Nalinakshi *et al* [14] analyzed numerically Double Diffusive mixed convection with variable fluid properties.

The main objective of the present investigation is to study systematically and numerically the Soret and Dufour effects on mixed convection heat and mass transfer for a Newtonian fluid flow past a semi infinite vertical heated plate embedded in a sparsely packed porous medium incorporating the variable porosity, permeability and thermal conductivity. To achieve this objective our plan of work is, in the analysis highly coupled non-linear partial differential equations governing the physical system are first reduced by a similarity transformations to the ordinary differential equations and then the resultant boundary value problem is converted into the system of seven simultaneous equations of first-order for seven unknowns. These equations are solved numerically by shooting technique by Runge-Kutta Methods to obtain velocity, temperature and concentration profiles for various physical parameters. The local Nusselt number and local Sherwood number variations are also shown graphically. The computed results here verify the accuracy of the method used under the limiting conditions which agree well with the existing ones.

2. MATHEMATICAL FORMULATION

A two-dimensional steady combined free-forced convective and mass transfer flow of a laminar, viscous, incompressible fluid over an isothermal semi-infinite vertical porous flat plate embedded in a sparsely packed porous medium of variable porosity, permeability and thermal conductivity is considered. The x-coordinate is measured along the plate from its leading edge, and y-coordinate normal to it. Let U_o be the velocity of the fluid in the upward direction and the gravitational field, g, is acting in the downward direction. The surface of the plate is maintained at a uniform constant temperature T_w and a uniform constant concentration C_w of a fluid, which are higher than the free stream values existing far away from the plate (i.e., $T_w > T_\infty$, $C_w > C_\infty$). It is also assumed that the free stream velocity U_0, parallel to the vertical plate, is constant.

Considering the theory of boundary layer effect for sparsely packed porous medium with high porosity ε (but less than unity), the general vectorial equations for the conservation of mass, momentum, energy and species concentration for steady, viscous, incompressible, Newtonian fluid flow can be written as:
Continuity equation:

$$\nabla.\vec{q} = 0, \tag{2.1}$$

Momentum equation:

$$\rho\left(\vec{q}.\nabla\right)\vec{q} = -\nabla p + \rho\vec{g}\,\beta_T\left(T-T_\infty\right) - \rho\vec{g}\,\beta_C\left(C-C_\infty\right) + \overline{\mu}\,\nabla^2\vec{q} - \frac{\mu\,\varepsilon}{k}\vec{q} - \varepsilon^2\frac{\rho\,C_b}{\sqrt{k}}\left|\vec{q}\right|\vec{q}, \tag{2.2}$$

Energy equation:

$$\left(\vec{q}.\nabla\right)T = \nabla.\left(\kappa\ \nabla T\right) + \phi + D_{12}\nabla^2 C, \tag{2.3}$$

Concentration equation:

$$\left(\vec{q}.\nabla\right)C = \kappa_S\nabla^2 C + D_{21}\nabla^2 T, \tag{2.4}$$

where $\vec{q} = (u, v)$, u and v are the velocity components along the x and y directions, respectively. ρ is the density of the fluid, $\vec{g}$ is the acceleration due to gravity, p is the pressure, T is the temperature of the fluid, C is the concentration of the fluid, $\overline{\mu}$ is the effective viscosity of the fluid, μ is the fluid viscosity, C_p is the specific heat at constant pressure, κ is the variable thermal conductivity, κ_S is the solutal diffusivity, β_T is the coefficient of volume expansion and β_C is the volumetric coefficient of expansion with species concentration. Equation (2.2) is the well-known Darcy-Brinkman equation which includes the boundary layer effect in the momentum equation. ϕ is the viscous dissipation term, D_{12} is the term caused by a concentration gradient (i.e., Dufour coefficient) and D_{21} is the term caused by a temperature gradient (i.e., Soret coefficient).

With the assumptions: (a) the Bousinesque approximation is valid i.e., density is constant everywhere in the momentum equation except in the buoyancy force (b) permeability, porosity and thermal resistance are functions of the vertical coordinate y, and (c) local thermal equilibrium exists between fluid and solid phase, the governing basic equations (2.1) – (2.4) for steady two-dimensional flow can be written in the form:
Continuity equation:

$$\frac{\partial u}{\partial x} + \frac{\partial u}{\partial y} = 0, \tag{2.5}$$

Momentum equation:

$$u\frac{\partial u}{\partial x} + v\frac{\partial u}{\partial y} = -\frac{1}{\rho}\frac{\partial p}{\partial x} + g\beta_T\left(T-T_\infty\right) - g\beta_C\left(C-C_\infty\right) + \frac{\overline{\mu}}{\rho}\frac{\partial^2 u}{\partial y^2} - \frac{\mu}{\rho}\frac{\varepsilon(y)}{k(y)}u - C_b\frac{\varepsilon^2(y)}{\sqrt{k(y)}}u^2, \tag{2.6}$$

Energy equation:

$$u\frac{\partial T}{\partial x} + v\frac{\partial T}{\partial y} = \frac{\partial}{\partial y}\left(\alpha(y)\frac{\partial T}{\partial y}\right) + \frac{\overline{\mu}}{\rho C_p}\left(\frac{\partial u}{\partial y}\right)^2 + \frac{D_m K_T}{C_s C_p}\frac{\partial^2 C}{\partial y^2} \tag{2.7}$$

Concentration equation:

$$u\frac{\partial C}{\partial x} + v\frac{\partial C}{\partial y} = \gamma^*\frac{\partial^2 C}{\partial y^2} + \frac{D_m K_T}{T_m}\frac{\partial^2 T}{\partial y^2}, \tag{2.8}$$

where $\phi = \frac{\overline{\mu}}{\rho C_p}\left(\frac{\partial u}{\partial y}\right)^2$, $D_{12} = \frac{D_m K_T}{C_s C_p}$, $D_{21} = \frac{D_m K_T}{T_m}$, $k(y)$ the variable permeability of the porous medium is, $\varepsilon(y)$ is the variable porosity of the saturated porous medium, $\alpha(y)$ is the variable effective thermal diffusivity of the medium and γ^* is the effective solutal diffusivity.

To determine the flow field the above governing equations need to be solved subject to the boundary conditions. The different types of rigid surfaces boundary conditions have been stated to describe flow characteristics at the boundary, near the plate and far away from the plate embedded in a sparsely packed porous medium. The following are the boundary conditions on velocity and temperature fields:

$$u = 0, \quad v = 0, \quad T = T_W, \quad C = C_W \quad \text{at} \quad y = 0, \tag{2.9}$$

$$u = U_o, \quad v = 0, \quad T = T_\infty, \quad C = C_\infty \quad \text{as} \quad y \to \infty, \tag{2.10}$$

Since the flow field is uniform at a sufficiently large distance from the porous surface, in the free stream $u = U_0$, where U_0 is the free stream velocity and T_∞ is the ambient temperature, then equation (2.6) reduces to

$$\frac{1}{\rho}\frac{\partial p}{\partial x} = -\frac{\mu\varepsilon(y)}{\rho k(y)}U_0, \tag{2.11}$$

Eliminating $\frac{\partial p}{\partial x}$ in equation (2.6) by using equation (2.11), we finally obtain the momentum equations as:

$$\begin{aligned} u\frac{\partial u}{\partial x} + v\frac{\partial u}{\partial y} = g\beta_T(T-T_\infty) - g\beta_C(C-C_\infty) + \frac{\overline{\mu}}{\rho}\frac{\partial^2 u}{\partial y^2} \\ + \frac{\mu}{\rho}\frac{\varepsilon(y)}{k(y)}(U_0 - u) + C_b\frac{\varepsilon^2(y)}{\sqrt{k(y)}}(U_0^2 - u^2), \end{aligned} \tag{2.12}$$

Equations (2.7), (2.8) & (2.12) are highly nonlinear partial differential equations, in order to solve them the following dimensionless variables f , θ and ϕ and as well as the similarity variable η are introduced (see Mohammadein and El-shaer [13]):

$$\eta = \left(\frac{y}{x}\right)\left(\frac{U_o x}{\nu}\right)^{1/2}, \quad \psi = \sqrt{\nu U_o x}\, f(\eta), \quad \theta = \frac{T-T_\infty}{T_w - T_\infty}, \quad \phi = \frac{C-C_\infty}{C_w - C_\infty} \tag{2.13}$$

the stream function $\psi(x, y)$ is defined by $u = \frac{\partial \psi}{\partial y}$, $v = -\frac{\partial \psi}{\partial x}$, such that the continuity equation (5) is satisfied automatically and the velocity components are given by

$$u = U_o f'(\eta), \quad v = -\frac{1}{2}\sqrt{\frac{\nu U_o}{x}}\left(f(\eta) - \eta f'(\eta)\right), \tag{2.14}$$

where, a prime represents differentiation with respect to η ,

Following Chandrashekhara and Namboodiri [7], the variable permeability $k(\eta)$, the variable porosity $\varepsilon(\eta)$ and variable effective thermal conductivity $\alpha(\eta)$ are given by

$$k(\eta) = k_o\left(1 + de^{-\eta}\right), \tag{2.15}$$

$$\varepsilon(\eta) = \varepsilon_o\left(1 + d^* e^{-\eta}\right), \tag{2.16}$$

$$\alpha(\eta) = \alpha_o[\varepsilon_o\left(1 + d^* e^{-\eta}\right) + \sigma^*\{1 - \varepsilon_o\left(1 + d^* e^{-\eta}\right)\}], \tag{2.17}$$

where k_o, ε_o and α_o are the permeability, porosity and thermal conductivity at the edge of the boundary layer respectively, σ^* is the ratio of the thermal conductivity of solid to the conductivity of the fluid, d and d^* are treated as constants having values 3.0 and 1.5 respectively for variable permeability and d = d*= 0 for uniform permeability.

Substituting (2.13) and (2.14) in Equations (2.7), (2.8) & (2.12) and using (2.15) – (2.17), we get the following transformed equations

$$f''' + \frac{1}{2}ff'' + \frac{Gr}{\mathrm{Re}^2}(\theta - N\phi) + \frac{\alpha^*\left(1 + d^* e^{-\eta}\right)}{\sigma\,\mathrm{Re}\left(1 + de^{-\eta}\right)}(1 - f') + \beta^*\frac{\left(1 + d^* e^{-\eta}\right)^2}{\left(1 + de^{-\eta}\right)^{1/2}}\left(1 - f'^2\right) = 0, \tag{2.18}$$

$$\theta'' = -\frac{\left(\frac{1}{2}\right)\mathrm{Pr}\,\theta' f + \mathrm{Pr}\,Ef''^2 + \varepsilon_o d^* e^{-\eta}\left(\sigma^* - 1\right)\theta' + \mathrm{Pr}\,Du\phi''}{\varepsilon_o + \sigma^*\left(1 - \varepsilon_o\right) + \varepsilon_o d^* e^{-\eta}\left(1 - \sigma^*\right)}, \tag{2.19}$$

$$\phi'' = -\left(\frac{1}{2}\right)Scf\phi' + ScSr\theta'' \tag{2.20}$$

where, $\mathrm{Pr} = \overline{\mu}/\rho\alpha_o$ is the Prandtl number, $Sc = \overline{\mu}/\rho\gamma_o$ is the Schmidt number, $\alpha^* = \mu/\overline{\mu}$ is the ratio of viscosities, $N = \frac{\beta_C(C_w - C_\infty)}{\beta_T(T_w - T_\infty)}$ is the Buoyancy ratio, $E = U_o^2/C_p(T_w - T_\infty)$ is the Eckert number, $\sigma = k_o/x^2\varepsilon_o$ is the local permeability parameter, $\mathrm{Re} = U_o x/\nu$ is the local Reynolds number, $\beta^* = C_b\frac{\varepsilon_o{}^2 x}{k_o{}^{1/2}}$ is the local inertial

parameter, $Gr_T = g\beta_T(T_w - T_\infty)x^3/\nu^2$ is the thermal Grashof number, $Gr_c = g\beta_C(C_w - C_\infty)x^3/\nu^2$ is the solutal Grashof number, $Du = \dfrac{D_m k_T(C_w - C_\infty)}{c_s c_p(T_w - T_\infty)}$ is the Dufour number and $Sr = \dfrac{D_m k_T(T_w - T_\infty)}{\nu \, \mathrm{T_m}(C_w - C_\infty)}$ is the Soret number. Here $Gr_T = Gr_C$.

The transformed boundary conditions are:

$$f = 0, \quad f' = 0, \quad \theta = 1, \quad \phi = 1 \quad \text{at} \quad \eta = 0 \tag{2.21}$$

$$f' = 1, \quad \theta = 0, \quad \phi = 0 \quad \text{as} \quad \eta \to \infty \tag{2.22}$$

once the velocity, temperature and concentration distributions are known, the skin friction and the rate of heat and mass transfer can be calculated respectively by

$$\tau = -f''(0)/\sqrt{\mathrm{Re}}, \quad Nu = -\sqrt{\mathrm{Re}}\,\theta'(0) \quad \text{and} \quad Sh = -\sqrt{\mathrm{Re}}\,\phi'(0) \tag{2.23}$$

where τ is the skin friction , Nu is the Nusselt number and Sh is the Sherwood number.

3 NUMERICAL METHOD

The boundary value problems arising due to vertical heated plate are highly coupled non linear equations which are difficult to solve analytically, hence numerical method by shooting technique is employed. Equations (2.18)-(2.20) with the boundary conditions (2.22) and (2.23) have been solved by using Newton-Raphson shooting technique along with Runge-Kutta fourth order integration scheme. Equations (2.19) - (2.21) constitute a highly non-linear coupled boundary value problem of third and second order respectively, they are transformed into system of simultaneous equations of first order. Further, they are transformed into initial value problem by applying shooting technique. The obtained initial value problem is then solved by employing Runge-Kutta fourth order integration scheme. The method is illustrated as given below:

1. Decision on ∞
2. Converting BVP to IVP by choosing suitable initial condition for $f, \theta \,\&\, \phi$
3. $f''(0), \theta'(0) \,\&\, \phi'(0)$ required for the solution of initial value problem are chosen by the classical, explicit Runge-Kutta method of fourth order.

The decision on an appropriate '∞' for the problem depends on the proper parameter values chosen. In view of this, for each parameter combination, the appropriate value of∞' has to be decided. The algorithm for the shooting method with Runge-Kutta fourth order approximating is used.

Initially, we chose guess values as $f''(0) = P,\ \theta'(0) = \mathrm{Q}$ and $\phi'(0) = \mathrm{R}.$. The process of obtaining P, Q & R accurately involves iteration process and can be calculated, repeating the same calculation we get another improved value, but these chosen guess values are not the most accurate values and hence there is a need to redefine. The better guess can be obtained by using the Newton-Raphson method. We solve the equations (2.19)-(2.21) with initial conditions

$$\begin{aligned} &f(0) = 0,\ f'(0) = 0,\ f''(0) = P, \\ &\theta(0) = 1,\ \theta'(0) = Q, \\ &\phi(0) = 1,\ \phi'(0) = \mathrm{R}. \end{aligned} \tag{3.1}$$

Due to crude choice of $f''(0), \theta'(0) \,\&\, \phi'(0)$, the solution at ∞' does not match with those given in the problem using the classical explicit Runge-Kutta method of fourth order. Thus, the coupled nonlinear boundary value problem of third-order in f and second-order in θ and ϕ has been reduced to a system of five simultaneous equations of first-order for five unknowns as follows :

$$\begin{aligned} f &= f_1, \\ \frac{df_1}{d\eta} &= f_2, \\ \frac{df_2}{d\eta} &= f_3, \end{aligned}$$

$$\frac{df_3}{d\eta} = -\frac{1}{2} f_1 f_3 - \frac{Gr}{\mathrm{Re}^2}\left(f_4 - Nf_7\right) - \frac{\alpha^*(1+d^*e^{-\eta})}{\sigma\,\mathrm{Re}(1+de^{-\eta})}(1-f_2) - \frac{\beta^*(1+d^*e^{-\eta})}{(1+de^{-\eta})^{1/2}}(1-f_2^{\,2}),$$

$$\theta = f_4,$$

$$\frac{df_4}{d\eta} = f_5,$$

$$\frac{df_5}{d\eta} = -\frac{(1/2)\,\mathrm{Pr}\, f_1 f_5 + \mathrm{Pr}\, Ef_3^{\,2} + \varepsilon_o d^* e^{-\eta}(\sigma^* - 1) f_5 + \mathrm{Pr}\, Duf_9}{\varepsilon_o + \sigma^*(1-\varepsilon_o) + \varepsilon_o d^* e^{-\eta}(1-\sigma^*)} = f_6$$

$$\phi = f_7,$$

$$\frac{df_7}{d\eta} = f_8,$$

$$\frac{df_8}{d\eta} = -\left(\frac{1}{2}\right) Scf_1 f_8 - ScSrf_6 = f_9, \tag{3.2}$$

where $f_1 = f,\ \ f_2 = f',\ f_3 = f'',\ \ f_4 = \theta,\ f_5 = \theta'\ ,\ f_7 = \phi,\ f_8 = \phi'$ and a prime denotes differentiation with respect to η.

The boundary conditions (2.21) and (2.22) now take the form

$$f_1(0) = 0,\ f_2(0) = 0,\ f_3(0) = \mathrm{P},\ f_4(0) = 1,\ f_5(0) = \mathrm{Q},\ f_7(0) = 1,\ f_8(0) = R \tag{3.3}$$

$$f_2(\infty) = 1,\ \mathrm{f}_4(\infty) = 0,\ \mathrm{f}_7(\infty) = 0. \tag{3.4}$$

To solve the system of first-order differential equations along with boundary conditions, we need seven initial conditions, but we have only two initial conditions on f, one initial condition on θ and one initial condition on ϕ. The third condition on $f\ \ (i.e.\, f''(0))$, second condition on $\theta(i.e.\theta'(0))$ and second condition on ϕ (i.e., $\phi'(0)$) are not prescribed, which are determined by employing numerical shooting method and using the ending boundary condition given in equation (3.4). The selection of an appropriate finite value of η_∞ is to be made. A good guess of the initial condition in the shooting technique is to be made on which the convergence depends. The accuracy of the assumed initial conditions is checked by comparing the calculated values of the dependent variable at the terminal point with its given value at that point. If any difference exists, improved values of the assumed initial conditions must be obtained and the process is repeated. The iterative process is terminated when the difference between two successive values reached 10^{-6}, then the solution is said to have converged results. The slight deviation in the values may be due to the use of Runge-Kutta-Fehlberg method which has fifth order accuracy whereas; Mohammadein and El-Shaer [13] have used fourth-order Runge-Kutta method which has only fourth order accuracy who has analysed the influence of variable permeability with heat transfer. Thus the present results are more accurate compared to their results.

4 RESULTS AND DISCUSSION

The system of first-order differential equations (3.2) are solved numerically using shooting technique with Runge-Kutta-Fehlberg method. In order to know the accuracy of the method used, computed values of $f''(0)$, $\theta'(0)$ and $\phi'(0)$ were obtained by varying the values of buoyancy ratio N, β*, $\alpha^*/\sigma\,\mathrm{Re}$, Gr/Re^2 for uniform permeability (d = 0.0, d^*= 0.0) and variable permeability (d=3.0, d^*=1.5) cases. The values are tabulated in Table 1 with few fixed values like $\varepsilon_o = 0.4, Ec = 0.1, \mathrm{Pr} = 0.71\ and\ \mathrm{Sc} = 0.22$.

A representative set of numerical results is shown graphically in Figures 1- 21, to illustrate the influence of physical parameters namely, Dufour and Soret number, the Richardson number Gr/Re^2, second order resistance β*, buoyancy ratio N, $\alpha^*/\sigma\,\mathrm{Re}$, Prandtl number Pr and Schmidt number Sc on the velocity, temperature and concentration. Also the variations of local Nusselt number and local Sherwood number are shown graphically.

For different values of the Dufour number D_f and Soret number S_r the velocity, temperature and concentration profiles are plotted in figures 1 - 3. The Dufour number D_f signifies the contribution of the concentration gradients to the thermal energy flux in the flow. The influence of Soret number S_r defines the effect of the temperature gradients inducing significant mass diffusion effects. It is observed that an increase in the Dufour number D_f and decrease in the Soret number S_r causes a rise in the velocity throughout the boundary layer as shown in figure 1. For D_f > 1, a distinct velocity overshoot exists near the plate, and thereafter the profile reaches the edge of the boundary layer. The increase in Dufour number D_f and decrease in Soret number S_r causes an increase of temperature throughout the boundary layer. For D_f < 1, the temperature profiles decay smoothly from the surface to the free stream value. However for D_f > 1, the temperature profile falls to zero at the edge of the boundary layer very rapidly as observed in Fig. 2. Fig. 3 demonstrates the dimensionless concentration for different values of Soret number S_r and Dufour number D_f. It is seen that concentration of the fluid increases within the boundary layer with decrease of Dufour number or increase of Soret number.

The effect of various values of N which defines the ratio of concentration buoyancy force to thermal buoyancy force parameters can be observed from Figs. 4 – 6. The Buoyancy ratio parameter N decreases the boundary layer increasing the velocity distributions significantly and decreases with temperature and concentration distributions. For fixed Dufour number $D_f = 2.0$ and Soret number $S_r = 0.03$ parameters, the velocity overshoot is observed for positive values of N ranging from 0 to 10, as N increases the overshoot increases. This is due to the fact that physically the assisting buoyancy force acts as a favourable pressure gradient which accelerates the fluid for lower Prandtl number Pr = 0.71causing the velocity profile within the boundary layer. This is observed in Fig. 4. The effects of N on the temperature and concentration profiles are very small due to the fact that the physical parameter N appears only in the momentum equation. Increase in the value of N decreases the temperature and concentration profiles.

The effect of different values of second order resistance β* which is expressed with the forchheimer term and the ratio of porosity to the permeability can be observed from Figs. 7- 9. The velocity distributions are shown in figure 7, increase in β* leads to increase in the velocity profiles. At β* = 0.0, the boundary layer shows the linear behavior and as β* increases the boundary layer shows the exponential form reaching far away from the plate. Fig. 8 and 9 depicts the temperature and concentration profiles for different values of β*. It is observed that as β* increases the temperature profiles decreases rapidly whereas the concentration profiles decreases proportionally with the increase of β*.

The mixed convection parameter i.e., the Richardson number Gr/Re^2 effects are shown in figures 10 to 12. Increase in the buoyancy force leads to higher Gr/Re^2 which accelerates the fluid leads the velocity closer to the vertical heated plate, and the free convection currents from the heated plate are carried away to the free stream with a downward acceleration acting leading the velocity to increase as observed in figure 10. Decrease in the parameter enhances the temperature and concentration in the boundary layer for both uniform and variable permeability cases as observed in figures 11 and 12. It is clearly observed that the variable permeability is little more dominant when compared to uniform permeability.

The effects of parameter $\alpha^*/\sigma\mathrm{Re}$ for velocity, temperature and concentration variations are shown in Figs. 13 to 15. Increase in the ratio of $\alpha^*/\sigma\mathrm{Re}$ leads to increase in the velocity profiles as shown in figure 13. This is due to the presence of low Reynolds number multiplied with ratio of viscosities resulting in the range of 0.0 to 0.5 in the momentum equation causing the velocity to overshoot increasingly. The variable permeability is more dominant compared to uniform permeability with the slight differences in the profiles. The effects of the parameter $\alpha^*/\sigma\mathrm{Re}$ on the temperature and concentration profiles as in observed in figures 14 and 15 are very small due to the fact that $\alpha^*/\sigma\mathrm{Re}$ appears only in the momentum equation. The temperature and concentration profiles decrease with increase in the parameter $\alpha^*/\sigma\mathrm{Re}$ and almost overlaps or very small difference with different increased value of $\alpha^*/\sigma\mathrm{Re}$ for both uniform and variable permeability cases.

The effects of Prandtl number Pr on velocity and temperature profiles are displayed in Figs. 16 and 17. Figure 16 shows the significant overshoot in the velocity profiles near the wall for lower Prandtl number fluid but for higher Prandtl number fluid the velocity overshoot is not much significant. The magnitude of the overshoot decreases as the Prandtl number increases. The effect is more in low Prandtl number fluid (air, Pr = 0.71) due to the low viscosity of the fluid, which increases the velocity within the boundary layer. The velocity profiles is not much significant for higher Prandtl number fluids (water, Pr = 7.0) because of more viscous fluid. The effects of Prandtl number Pr results into the

thinner thermal boundary layer as the higher Prandtl number has a lower thermal conductivity as shown in figure 17. The variations in the concentration profiles due to the effects of Prandtl number Pr are very less, hence the variations in the concentration profiles for the effects of Schmidt number Sc are displayed in figure 18. Increase in the Schmidt number Sc results in decrease of the concentration profiles. The effect of Schmidt number is not very prominent on temperature distribution for different values of Sc.

The variations in temperature profiles for different values of σ* are displayed in 19. Increase in σ* leads to decrease in thermal boundary layer due to higher thermal conductivity. The variations of the Nusselt number and Sherwood number as a function of for various D_f values of S_r are shown in Figs. 20 and 21. Figure 20 describes the behavior of local Nusselt number with changes in the values of D_f and S_r. It is observed that the effect of increasing D_f is to increase the Nusselt number for the increasing values of S_r for both uniform and variable permeability cases. From figure 21, it is observed that the values of local Sherwood number increase with increase in the value of S_r for both uniform and variable permeability cases. Also, higher the value of S_r, greater its effect on Sherwood number for all values of D_f as observed in the figure 21 i.e., the effect of Dufour number on Sherwood number is appreciable in the solutal boundary layer, which increases with increase in the Dufour number.

5 CONCLUSIONS

The problem of steady laminar, viscous, incompressible two-dimensional mixed convection flow due to vertical heated plate embedded in a Newtonian fluid sparsely packed porous medium in the presence of Soret and Dufour effects with variable fluid properties such as variable porosity, permeability and thermal conductivity is investigated. The resulting partial differential equations, describing the problem, are transformed into ordinary differential equations by using similarity transformations. These equations are more conveniently solved numerically by Runge-Kutta-Fehlberg method with shooting technique for the computation of fluid flow, heat and mass transfer characteristics, skin-friction coefficient, heat transfer rate and mass transfer rate for various values of the Soret and Dufour number, Buoyancy ratio, second order resistance, mixed convection parameter, ratio of viscosities to Reynolds number, etc. for both uniform permeability and variable permeability cases. Comparisons of the present results with previously published works on limiting cases in the absence of many parameters but with the variable fluid properties as shown in chapter 3 were performed and results were found to be in excellent agreement. From this investigation the following conclusions are drawn:

(i) Increase in the mixed convection parameter Gr/Re^2 increases the fluid flow velocity near the vertical heated plate in the momentum boundary layer and slowly asymptotes towards the free stream, whereas its effect is reversed in the thermal and solutal boundary layer as the Gr/Re^2 parameter increases.

(ii) Velocity increases with the increase of Dufour number (and decrease of Soret number), whereas decrease in Dufour number (increase of Soret number) leads to decrease the temperature and increase in Dufour number (decrease of Soret number) leads to decrease in concentration.

(iii) As the Buoyancy ratio N increases the velocity increases, temperature profiles decreases and concentration decreases.

(iv) The increase in the non-Darcy parameter β^*, implies that the porous medium is offering more resistance to the fluid flow, hence velocity increases as we increase the parameter and temperature and concentration decreases as we increase the parameter.

(v) Increase in Prandtl number leads to decrease in the velocity profiles, it is observed that at low Prandtl number the velocity overshoot is more significant. The temperature profiles are decreasing with the increase in Prandtl number. It is found that the concentration profiles decreases with increasing the values of Schmidt number Sc due to decrease in the solutal boundary layer thickness.

(vi) Local Nusselt number decreases with decrease in the value of Soret number as the Dufour number increases.

Table 1 Results for $f''(0),\ -\theta'(0)$ and $-\phi'(0)$ for $\Pr = 0.71,\ Sc = 0.22,\ Ec = 0.1,\ \varepsilon_o = 0.4$ for Uniform Permeability (UP) and Variable Permeability (VP) cases.

D_f, S_r	N		Gr/Re^2	$\alpha^*/\sigma Re$	β^*	Uniform Permeability (UP)			Variable Permeability (VP)		
						$f''(0)$	$-\theta'(0)$	$-\phi'(0)$	$f''(0)$	$-\theta'(0)$	$-\phi'(0)$
2.00,0.03	1	2	0.2	0.1	0.0	0.449345	0.378450	0.377500	0.452345	0.381450	0.378500
					0.1	0.464565	0.394567	0.390004	0.474565	0.404567	0.393564
					0.5	0.554567	0.438780	0.429500	0.564567	0.441780	0.436500
					1.5	0.647800	0.507030	0.499900	0.657800	0.510030	0.509900
				0.0	0.1	0.423450	0.351340	0.348020	0.433450	0.361340	0.350020
				0.1		0.464565	0.394567	0.390004	0.474565	0.404567	0.393564
				0.5		0.534560	0.458250	0.457210	0.554560	0.463450	0.461110
			0.0	0.1	0.1	0.397800	0.279800	0.273700	0.367800	0.291340	0.281780
			0.2			0.464565	0.394567	0.390004	0.474565	0.404567	0.393564
			1.0			0.715650	0.518900	0.500050	0.720050	0.502903	0.491050
			2.0			0.843560	0.541250	0.538500	0.851260	0.540250	0.531200
		2.0	0.2	0.1	0.1	0.464565	0.394567	0.390004	0.474565	0.404567	0.393564
		4.0				0.495678	0.411780	0.408010	0.501548	0.423280	0.410010
		6.0				0.552453	0.431789	0.425897	0.569870	0.443219	0.433164
	0.0	2.0	0.2	0.1	0.1	0.399450	0.312450	0.310010	0.401250	0.323900	0.320010
	1.0					0.464565	0.394567	0.390004	0.474565	0.404567	0.393564
	5.0					0.745640	0.441890	0.440010	0.731240	0.450018	0.448410
	10.0000000					0.889070	0.491050	0.491550	0.895070	0.509070	0.498550
2.00,0.03	1.0	2.0	0.2	0.1	0.1	0.464565	0.394567	0.390004	0.474565	0.404567	0.393564
1.00,0.06						0.481120	0.400250	0.399500	0.483120	0.413453	0.400134
0.40,0.15						0.494500	0.416700	0.412020	0.498500	0.420054	0.418945
0.15,0.40						0.528900	0.421890	0.420040	0.531670	0.429918	0.427896
0.06,1.00						0.548965	0.434560	0.430010	0.557891	0.438763	0.433981
0.03,2.00						0.565678	0.451780	0.449010	0.569821	0.463789	0.457654

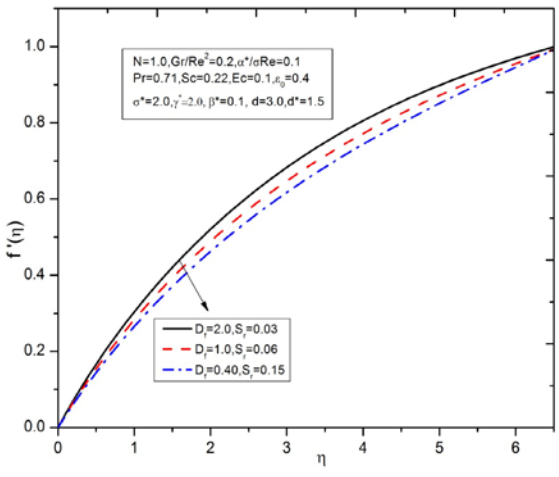

Fig. 1 Velocity profiles for different values of Soret and Dufour numbers for VP case

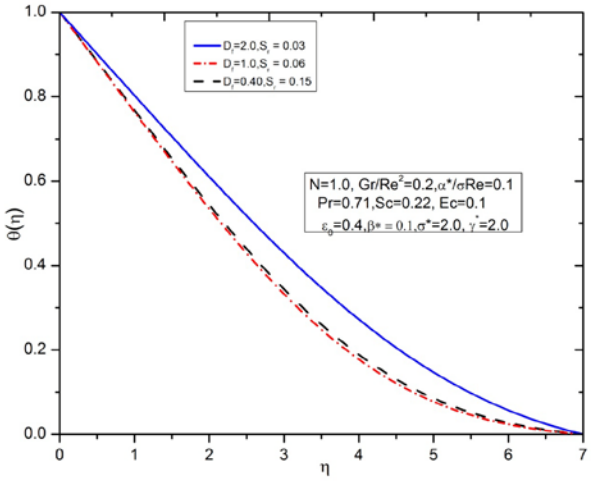

Fig. 2 Temperature profiles for different values of Soret and Dufour numbers for VP case

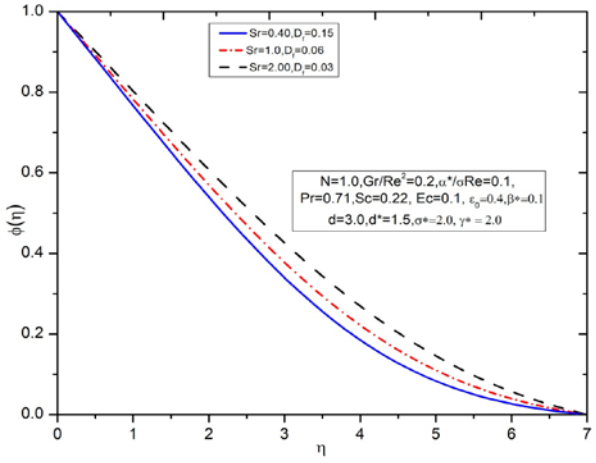

Fig. 3 Concentration profiles for different values of Soret and Dufour numbers for VP case

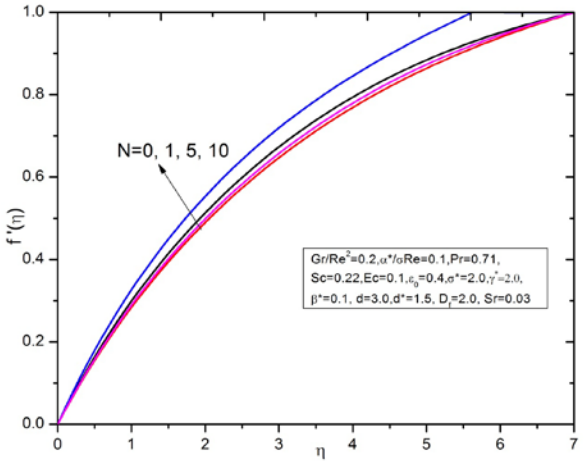

Fig. 4 Velocity profiles for different value of buoyancy ratio N for VP case

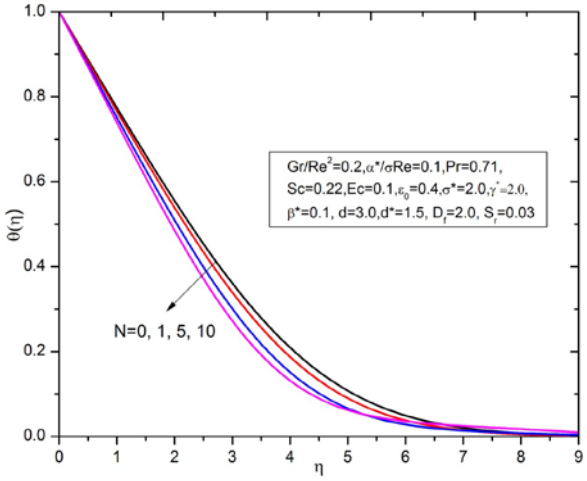

Fig. 5 Temperature profiles for different values of buoyancy ratio N for VP case

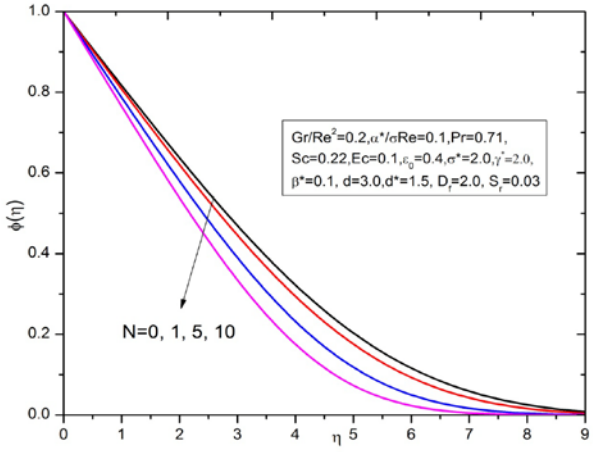

Fig. 6 Concentration profiles for different values of buoyancy ratio N for VP case

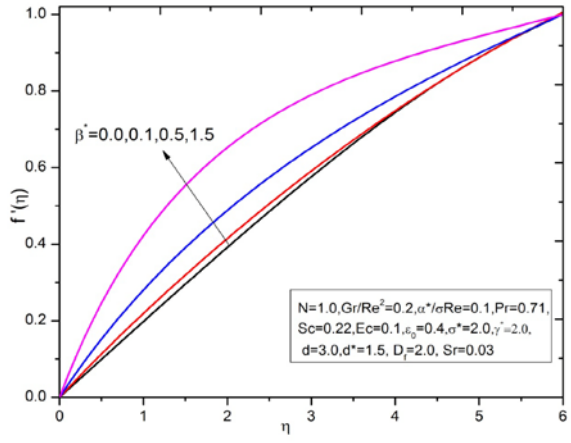

Fig. 7 Velocity variations for various values of second order resistance $\beta *$ for VP case

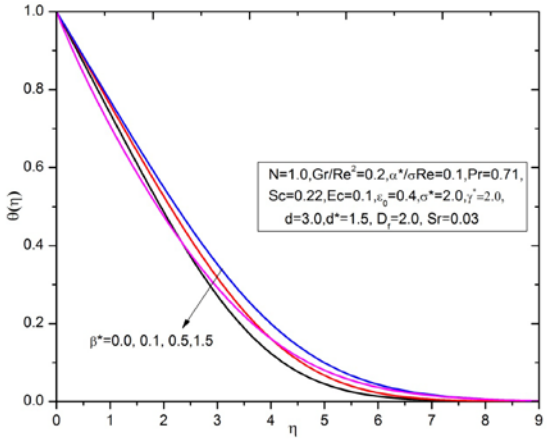

Fig. 8 Temperature variations for various values of second order resistance $\beta *$ for VP case

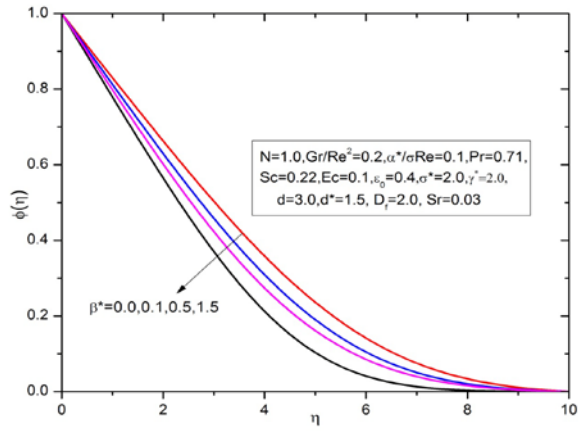

Fig. 9 Concentration variations for various values of second order resistance β^* for VP case

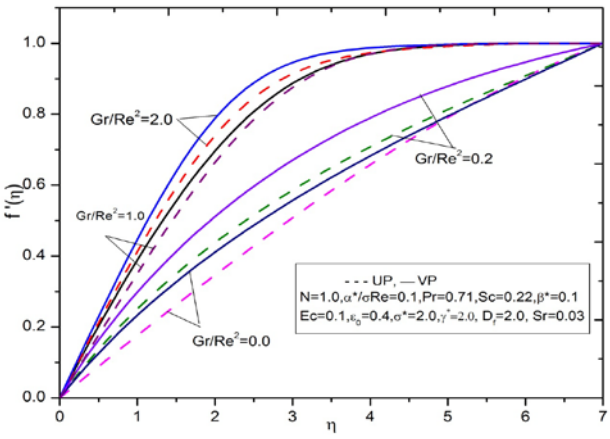

Fig. 10 Velocity distributions for different values of Gr/Re^2 for UP and VP cases

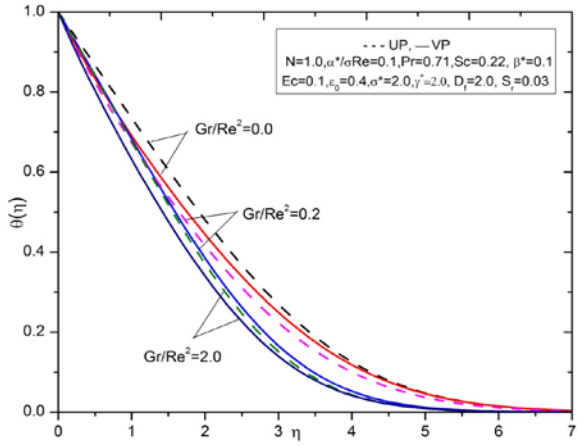

Fig. 11 Temperature distributions for different values of Gr/Re^2 for UP and VP cases

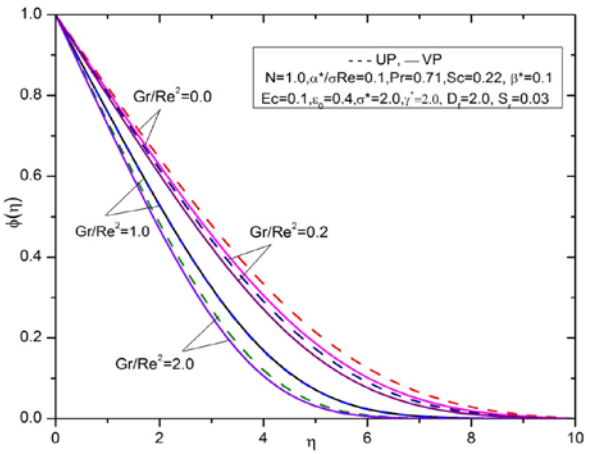

Fig. 12 Concentration distributions for different values of Gr/Re^2 for UP and VP cases

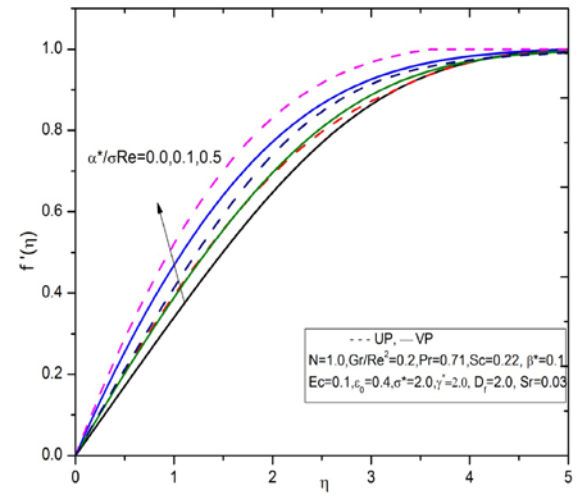

Fig. 13 Velocity profiles for various values of $\alpha^*/\sigma\,\mathrm{Re}$ for UP and VP cases

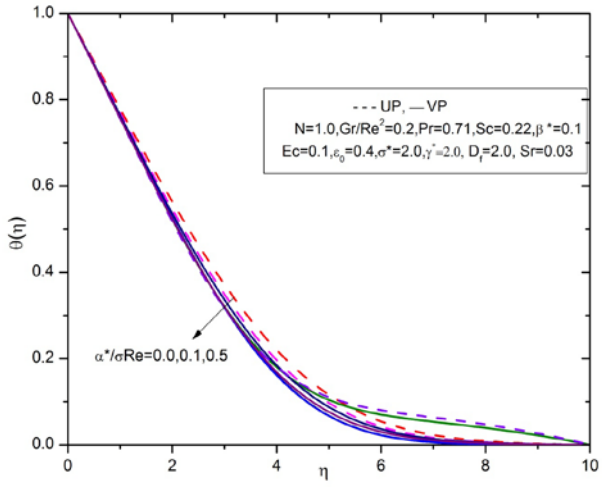

Fig. 14 Temperature profiles for various values of $\alpha^*/\sigma\,\mathrm{Re}$ for UP and VP cases

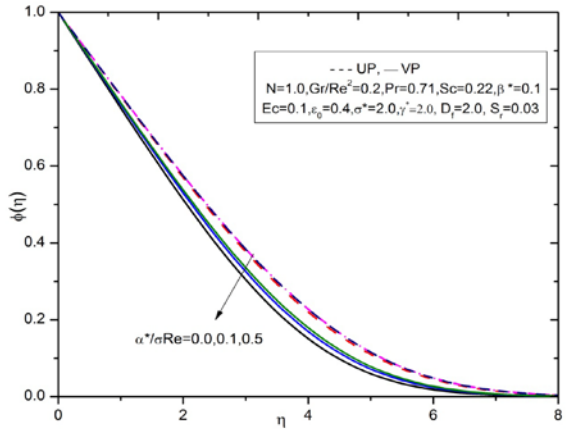

Fig. 15 Concentration profiles for various values of α^* / σ Re for UP and VP cases

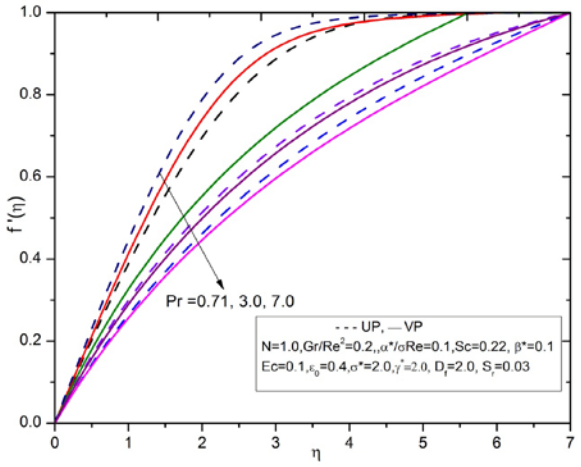

Fig. 16 Velocity profiles for various values of Pr for UP and VP cases

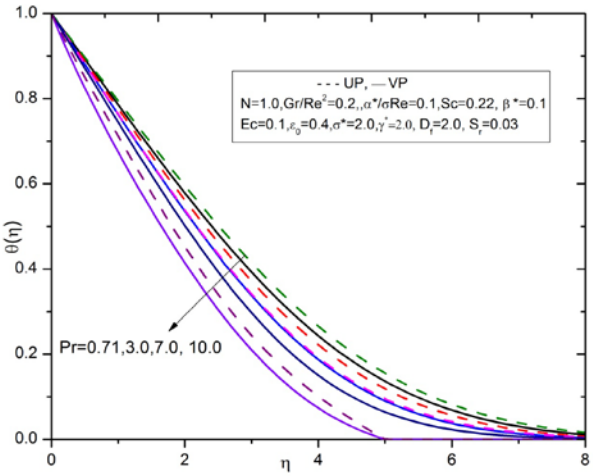

Fig. 17 Temperature profiles for various values of Prandtl number Pr for UP and VP case

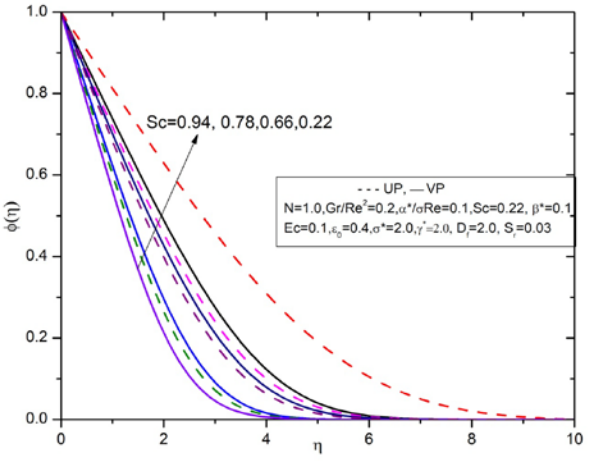

Fig. 18 Concentration profiles for various values of Schmidt number Sc for UP and VP cases

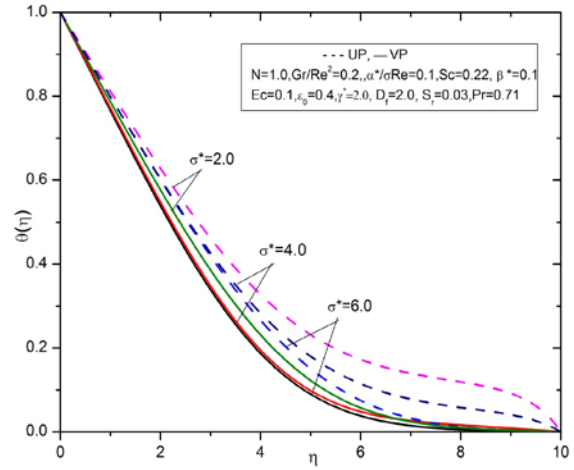

Fig. 19 Temperature profiles for various values of σ*for UP and VP cases

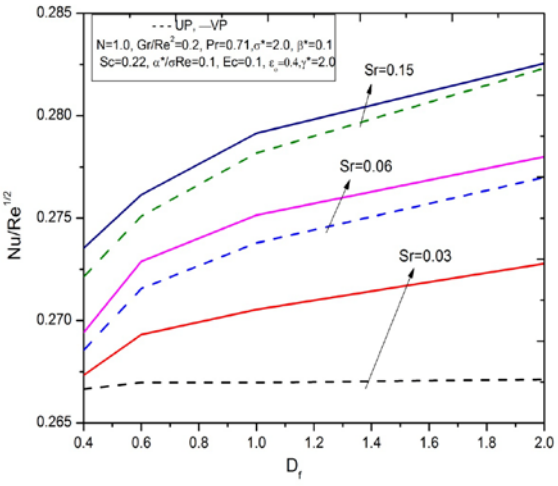

Fig. 20 Variations in local Nusselt number with D_f for various values of S_r for UP and VP cases

6. REFERENCES

[1] Alam M.S., Rahman M.M., "Dufour and Soret effects on mixed convection flow past a vertical porous flat plate with variable suction", Nonlinear Analysis: Modelling and Control, vol.11(1), (2006), 3-12.

[2] Anghel M., Takhar H.S., and Pop I., Dufour and Soret effects on free convection boundary layer over a vertical surface embedded in a porous medium, J Heat and Mass Transfer, vol.43, (2000), 1265-1274.

[3] Awad F.G., Sibanda P., and Sandile Motsa S., On the linear stability analysis of a Maxwell fluid with double-diffusive convection, Applied Mathematical Modelling 34**,** (2010), 3509-3517.

[4] Balasubrahmanyam M., Sudarshan Reddy P., and Sivaprasad R., Soret effect on Mixed convective heat and mass transfer through a porous medium confined in a cylindrical annulus under a radial magnetic field in the presence of a constant heat sourc/sink, Int. J. of Appl. Math and Mech 7(8), (2011), 1-17.

[5] Benanati R.F., and Brosilow C.B., Void fraction distribution in beds of spheres, AIChe. J., vol.8, (1962), 359-361.

[6] Chandrasekhara B.C., Namboodiri P. M. S., and Hanumanthappa A. R., Similarity solutions of buoyancy induced flows in a saturated porous medium adjacent to impermeable horizontal surfaces, Warme Stoffubertrag. 18, (1984), 17-23.

[7] Chandrasekhara B.C., and Namboodiri P.M.S., Influence of variable permeability on combined vertical surfaces in porous medium, International Journal of Heat Mass Transfer, vol.28, (1985), 199-206.

[8] Dulal Pal., Magnetohydrodynamic non-Darcy mixed convection heat transfer from a vertical heated plate embedded in a porous medium with variable porosity, Commun Nonliner Sci Numer Simulat, Vol.15, (2010), 3974-3987.

[9] Eckert E.R.G., and Drake R.M., Analysis of Heat and Mass Transfer, New York, McGraw-Hill Book (1972).

[10] Gnaneswara Reddy, and Bhaskar Reddy, Soret and Dufour Effects on steady MHD Free Convection Flow past a Semi-infinite Moving Vertical Plate in a Porous Medium with Viscous Dissipation, Int. J. of Appl. Math and Mech., 6(1), (2010), 1-12.

[11] Gnaneswara Reddy, and Bhaskar Reddy, Finite element analysis of Soret and Dufour effects on unsteady MHD free convection flow past an impulsively started vertical porous plate with viscous dissipation, Journal of Naval Architecture and Marine Engineering 8, (2011), 1-12.

[12] Govardhan K., Balaswamy B., and Kishan N., Effects of Internal Heat Generation, Soret and Dufour effects on MHD Free Convection Heat and Mass Transfer in a Doubly Stratified Darcy Porous Medium with Viscous Dissipation, Emirates Journal of Engineering Research, 17(2), (2012), 29-42.

[13] Mohammadein A. A., and EL-SHAER N. A., Influence of variable permeability on combined free and forced convection flow past a semi-infinite vertical plate in a saturated porous medium, Heat Mass Transfer, vol.40,(2004), 341-346.

[14] Nalinakshi N., Dinesh P.A., and Chandrashekhar D.V., "Numerical Study of Double Diffusive Mixed Convection with variable Fluid properties" Intl. J. Engng. Res. & Tech., volume 2, Issue 9, (2013), pp. 131-139.

[15] Nield D. A., and Bejan A., Convection in porous media, Springer-Verlag, (1991).

[16] Pal D., and Shivakumara I S., Mixed Convection heat transfer from a vertical heated plate embedded in a sparsely packed porous medium, Int. J. Appl. Mech. Eng., 11, (2006), 929-939.

[17] Postelnicu A., Influence of a magnetic field on heat and mass transfer by natural convection from vertical surfaces in porous media considering Soret and Dufour effects, Int. J. Heat Mass Transfer, 47,(2004),1467-1472.

[18] Schwartz C. E., and Smith J. M., Flow distribution in packed beds, Ind. Eng. Chem., vol.45, (1953), 1209-1218.

Source of support: Nil, Conflict of interest: None Declared

